MOZ and BMI1 play opposing roles during *Hox* gene activation in ES cells and in body segment identity specification in vivo

Bilal N. Sheikh[a,b], Natalie L. Downer[a], Belinda Phipson[c], Hannah K. Vanyai[a,b], Andrew J. Kueh[a], Davis J. McCarthy[c], Gordon K. Smyth[c,d], Tim Thomas[a,b,1,2], and Anne K. Voss[a,b,1,2]

[a]Development and Cancer Division, The Walter and Eliza Hall Institute of Medical Research, Melbourne, VIC 3052, Australia; [b]Department of Medical Biology, University of Melbourne, Melbourne, VIC 3052, Australia; [c]Bioinformatics Division, The Walter and Eliza Hall Institute of Medical Research, Melbourne, VIC 3052, Australia; and [d]Department of Mathematics and Statistics, University of Melbourne, Melbourne, VIC 3052, Australia

Edited by Clifford J. Tabin, Harvard Medical School, Boston, MA, and approved March 23, 2015 (received for review December 1, 2014)

Hox **genes underlie the specification of body segment identity in the anterior–posterior axis. They are activated during gastrulation and undergo a dynamic shift from a transcriptionally repressed to an active chromatin state in a sequence that reflects their chromosomal location. Nevertheless, the precise role of chromatin modifying complexes during the initial activation phase remains unclear. In the current study, we examined the role of chromatin regulators during *Hox* gene activation. Using embryonic stem cell lines lacking the transcriptional activator MOZ and the polycomb-family repressor BMI1, we showed that MOZ and BMI1, respectively, promoted and repressed *Hox* genes during the shift from the transcriptionally repressed to the active state. Strikingly however, MOZ but not BMI1 was required to regulate *Hox* mRNA levels after the initial activation phase. To determine the interaction of MOZ and BMI1 in vivo, we interrogated their role in regulating *Hox* genes and body segment identity using *Moz;Bmi1* double deficient mice. We found that the homeotic transformations and shifts in *Hox* gene expression boundaries observed in single *Moz* and *Bmi1* mutant mice were rescued to a wild type identity in *Moz;Bmi1* double knockout animals. Together, our findings establish that MOZ and BMI1 play opposing roles during the onset of *Hox* gene expression in the ES cell model and during body segment identity specification in vivo. We propose that chromatin-modifying complexes have a previously unappreciated role during the initiation phase of *Hox* gene expression, which is critical for the correct specification of body segment identity.**

MYST | histone acetyltransferase | lysine acetyltransferase | BMI1 | polycomb

Hox genes specify cell identity in the anterior–posterior axis in bilaterian organisms (1). Mammals possess four paralogous *Hox* gene clusters, *Hox A*, *B*, *C*, and *D*, which display unique collinearity in their expression. *Hox* genes present at the 3′ end of *Hox* clusters are activated first during gastrulation and specify the most anterior segments of the body, whereas the more 5′ genes are sequentially activated and specify more posterior segments in a chronological manner (2–4). Once the initial activation phase of *Hox* genes is complete, *Hox* gene expression boundaries are fine-tuned. This phase is followed by the maintenance of *Hox* gene expression domains at specific anterior-to-posterior levels that are propagated through development and into adulthood via epigenetic mechanisms (5).

Hox gene activation involves dynamic changes in chromatin structure. Before activation, *Hox* loci in mouse embryos in vivo (6) and in ES cells (7, 8) remain in a chromatin state that is poised for transcriptional activation. This state is characterized by the combined presence of histone modifications that are typical of both transcriptionally active and repressed chromatin, e.g., H3K4me3 and H3K27me3, a state termed bivalent. During collinear activation of *Hox* genes, active chromatin marks such as H3K4me3 and H3 acetylation spread through the *Hox* clusters in a 3′ to 5′ direction mirroring the activation of *Hox* mRNA expression (9). Concurrently, there is a shift in 3D domain structure of *Hox* loci, whereby active *Hox* loci are segregated into a separate topological domain compared with bivalently marked, transcriptionally repressed *Hox* loci (6, 10). Despite the highly dynamic nature of chromatin during *Hox* gene activation, the importance of chromatin modifying complexes during the initial shift from a repressed to transcriptionally active state remains enigmatic. Indeed, it is generally thought that chromatin-modifying complexes only play an important role in the maintenance phase of *Hox* gene expression, and not during their initial activation (11, 12).

In the current study, we set out to investigate the importance of chromatin modifiers in regulating the onset of *Hox* gene expression. To establish an experimental system where we could investigate the balance between transcriptional activation versus repression at *Hox* loci, we focused on the concurrent activities of the transcriptional activator monocytic leukemia zinc finger protein (MOZ, MYST3, KAT6A) (13), and the polycomb-group transcriptional repressor BMI1 (14). MOZ is the catalytic unit of a four-member molecular complex (15, 16), that is required for H3K9 acetylation at *Hox* loci in vivo (13). In contrast, BMI1 is a member of the polycomb repressive complex 1 (PRC1) which ubiquitinates (ub) H2AK119 via its catalytic units RING1A/RING1B (14, 17, 18). Interestingly, although PRC1-mediated H2AK119ub is considered important for restraining premature

Significance

The body is patterned in the anterior–posterior axis by the correct spatial and temporal expression of *Hox* genes during embryonic development. One mechanism critical for the precise spatiotemporal expression of *Hox* genes is the chromatin state. While changes in chromatin conformation during the activation of *Hox* genes have been well described, the importance of the factors that in turn regulate chromatin remains enigmatic and controversial. In the current study, we investigate the role of two critical chromatin regulators, MOZ and BMI1, during *Hox* gene activation and in specifying body segment identity. We establish the importance of MOZ and BMI1 during the initial activation of *Hox* genes in ES cells and in correctly specifying body segment identity during embryonic development.

Author contributions: B.N.S., T.T., and A.K.V. designed research; B.N.S., N.L.D., H.K.V., and A.J.K. performed research; B.N.S., B.P., H.K.V., D.J.M., G.K.S., T.T., and A.K.V. analyzed data; and B.N.S., T.T., and A.K.V. wrote the paper.

The authors declare no conflict of interest.

This article is a PNAS Direct Submission.

Freely available online through the PNAS open access option.

[1]T.T. and A.K.V. contributed equally to this work.

[2]To whom correspondence may be addressed. Email: avoss@wehi.edu.au or tthomas@wehi.edu.au.

This article contains supporting information online at www.pnas.org/lookup/suppl/doi:10.1073/pnas.1422872112/-/DCSupplemental.

DEVELOPMENTAL BIOLOGY

activation of bivalently marked genes in ES cells (19, 20) and for maintaining ES cell identity (19), it appears to be dispensable for chromatin compaction imparted by the PRC1 complex (19, 21). Consistent with their importance in the regulation of *Hox* genes, mice lacking MOZ display an extensive anterior homeotic transformation along with a 50% decrease in *Hox* mRNA levels (13). Conversely, mice lacking BMI1 display a posterior homeotic transformation of the axial skeleton (22, 23).

In this study, we established ES cell lines singly or doubly deficient in MOZ and BMI1 to model early events during the activation of *Hox* genes. Through the interrogation of temporal *Hox* gene expression dynamics, we show that MOZ and BMI1 control the balance between activation and repression in the period before and during *Hox* activation. Thereafter, MOZ but not BMI1 was critical for the maintenance of normal transcription levels. To investigate the functional interplay of MOZ and BMI1 in vivo, we undertook an analysis of body segment identity in *Moz* and *Bmi1* single and double knockout mice. We show that the extensive defects in *Hox* gene expression domains and homeotic transformations observed in *Moz* and *Bmi1* single mutants were rescued in *Moz*;*Bmi1* double mutant mice. Thus, through our analysis of MOZ and BMI1, we expose the importance of chromatin modifying complexes during *Hox* gene activation in ES cells and in regulating body segment identity in vivo.

Results

MOZ and BMI1 Are Expressed During Gastrulation and in Early Somites. To investigate the importance of chromatin modifying complexes during the onset of *Hox* gene expression, we focused on the interplay between a transcriptional activator of *Hox* genes, MOZ, and a transcriptional repressor, BMI1. Foremost, we determined if *Moz* and *Bmi1* were expressed in the region surrounding the primitive streak, where *Hox* gene expression is first specified during gastrulation. We isolated wild type embryos between embryonic day (E) 7.5 and E10.5 and assayed the expression patterns of *Moz* and *Bmi1* mRNA by whole mount in situ hybridization.

In the E7.5 embryo, both *Moz* and *Bmi1* were expressed in the chorionic plate trophectocerm (*SI Appendix*, Fig. S1). In addition, *Moz* and *Bmi1* expression was observed around the primitive streak and in the presomitic mesoderm (Fig. 1 *A* and *B*). At E8.5, *Moz* and *Bmi1* expression was observed in the somites and the receding primitive streak region (Fig. 1 *C* and *D*). In addition, *Moz* was expressed in the facial region and the anterior pharyngeal arches, an area where MOZ is required for normal levels of *Tbx1* gene expression during development (24). At E9.5 and E10.5, *Moz* was ubiquitously expressed (Fig. 1 *E* and *G*), consistent with its continued requirement for maintaining gene expression. In contrast, only low levels of *Bmi1* mRNA were observed by E10.5 (Fig. 1*H*). Thus, our qualitative analysis of *Moz* and *Bmi1* mRNA expression reveal that both chromatin regulators could play an important role during the onset of *Hox* gene expression.

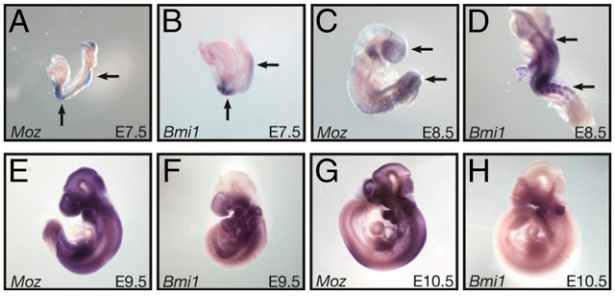

Fig. 1. *Moz* and *Bmi1* are expressed during the *Hox* gene activation phase in vivo. (*A* and *B*) *Moz* and *Bmi1* mRNAs were detected in the area of the somites and the receding primitive streak in the head fold-stage embryo. (*C*) *Moz* mRNA is expressed in the neural tube, facial structures, pharyngeal arches, and somites at E8.5. (*D*) *Bmi1* mRNA was detected in the hindbrain rhombomeres, the trunk neural tube, facial structures, pharyngeal arches, and somites at E8.5. (*E* and *F*) *Moz* and *Bmi1* mRNAs are widely expressed at E9.5. (*G*) *Moz* mRNA expression was extensively detected at E10.5. (*H*) Weak ubiquitous *Bmi1* mRNA expression is evident at E10.5. n = 3–5 wild-type embryos per probe at each stage. See related data in *SI Appendix*, Fig. S1.

$Moz^{\Delta/\Delta}$;$Bmi1^{-/-}$ Double Mutant Embryos Display Edema and Die Between E15.5 and E18.5. To investigate the relationship between MOZ and BMI1, we crossed Moz^{Δ} mice (25) and $Bmi1^{-}$ mutant mice (23). Intercrosses of $Moz^{\Delta/+}$;$Bmi1^{+/-}$ produced offspring of all nine expected genotypes at normal Mendelian frequencies at embryonic day (E) 10.5, E12.5 and E15.5 (*SI Appendix*, Table S1, $P > 0.50$, χ^2 test). A large proportion of $Moz^{\Delta/\Delta}$;$Bmi1^{-/-}$ fetuses presented with edema at E15.5 and only two living $Moz^{\Delta/\Delta}$;$Bmi1^{-/-}$ pups were isolated at E18.5, which was significantly less than the expected number ($P = 0.026$, χ^2 test). This suggests that $Moz^{\Delta/\Delta}$;$Bmi1^{-/-}$ fetuses die between E15.5 and E18.5.

BMI1 Restrains Premature Activation of *Hox* Genes in ES Cells. To investigate the role of MOZ and BMI1 during the early phase of *Hox* gene activation, we established ES cell lines from E3.5 blastocysts from $Moz^{\Delta/+}$;$Bmi1^{+/-}$ intercrosses (Fig. 2*A*). There was no difference in the expression of pluripotency markers *Oct4* and *Nanog* in *Moz*;*Bmi1* compound knockout ES cells (*SI Appendix*, Fig. S2 *A* and *B*). As expected, no *Moz* mRNA was detected in ES cells lacking the *Moz* gene (*SI Appendix*, Fig. S2*C*), and no *Bmi1* mRNA was evident in $Bmi1^{-/-}$ ES cells (*SI Appendix*, Fig. S2*D*).

Hox genes are expressed at low, but detectable levels in ES cells compared with embryonic forebrain tissue where they are inactive (6). To determine the effects of MOZ and BMI1 on *Hox* genes prior to retinoic acid (RA)-induced activation, we analyzed *HoxA* cluster expression levels in *Moz*;*Bmi1* ES cells. There was a significant increase in the expression of *HoxA* cluster genes in $Bmi1^{-/-}$ ES cells compared with wild type (Fig. 2*C*, $P = 0.015$). In contrast, ES cells lacking *Moz* displayed the opposing phenotype, with a decrease in *HoxA* cluster expression ($P = 0.008$). These data are consistent with ascribed roles of MOZ and the BMI1-PRC1 complex in transcriptional regulation (13, 14, 24, 26). Interestingly, in $Moz^{\Delta/\Delta}$;$Bmi1^{-/-}$ ES cells, the effects of *Bmi1* deletion and not the effects of *Moz*-deletion were observed. *HoxA* cluster genes were significantly over-expressed in $Moz^{\Delta/\Delta}$;$Bmi1^{-/-}$ ES cells compared with wild type ($P = 0.04$) and compared with $Moz^{-/-}$ ES cells ($P < 0.001$). Indeed, the expression of *HoxA* cluster genes in $Moz^{\Delta/\Delta}$;$Bmi1^{-/-}$ ES cells was similar to that of $Bmi1^{-/-}$ cells ($P = 0.746$). These data indicate that the repression implemented by BMI1 is particularly important to maintain *Hox* genes in a transcriptionally repressed state and inhibit their premature activation in ES cells.

MOZ and BMI1 Play Opposing Roles During RA-Induced Activation of *Hox* Genes. To determine the effects of MOZ and BMI1 during the early phase of *Hox* gene activation, we induced *Moz*;*Bmi1* ES cells to differentiate with RA. We used physiological levels of RA (20 nM), as it is critical for ensuring that *Hox* gene activation does not exceed the extend and amplitude of *Hox* gene activation observed in vivo (27). Two hours of RA treatment resulted in strong induction of *Hoxa1*, *Hoxa3* and *Hoxa5*, with their mRNA 10–20 fold more abundant compared with levels in undifferentiated ES cells (Fig. 2*B*). By 12 h, the 3′ *HoxA* cluster genes, namely *Hoxa1*, *Hoxa2*, *Hoxa3*, *Hoxa4*, *Hoxa5* and *Hoxa6* were strongly activated, with expression of *Hoxa3* as much as 200-fold more abundant than in undifferentiated ES cells (Fig. 2*B*). In contrast, *Hox* genes at the 5′ end of the *HoxA* cluster continued to be expressed at low levels. These data indicate that ES cells of all genotypes underwent collinear activation of *Hox* genes over a 12 h time period in response to RA.

Next, we quantitatively compared the levels of *HoxA* cluster mRNA between *Moz* and *Bmi1* deficient cells. At the two-hour time point, the absence of BMI1 produced a strong effect. In comparison with wild type, *HoxA* cluster genes were expressed at

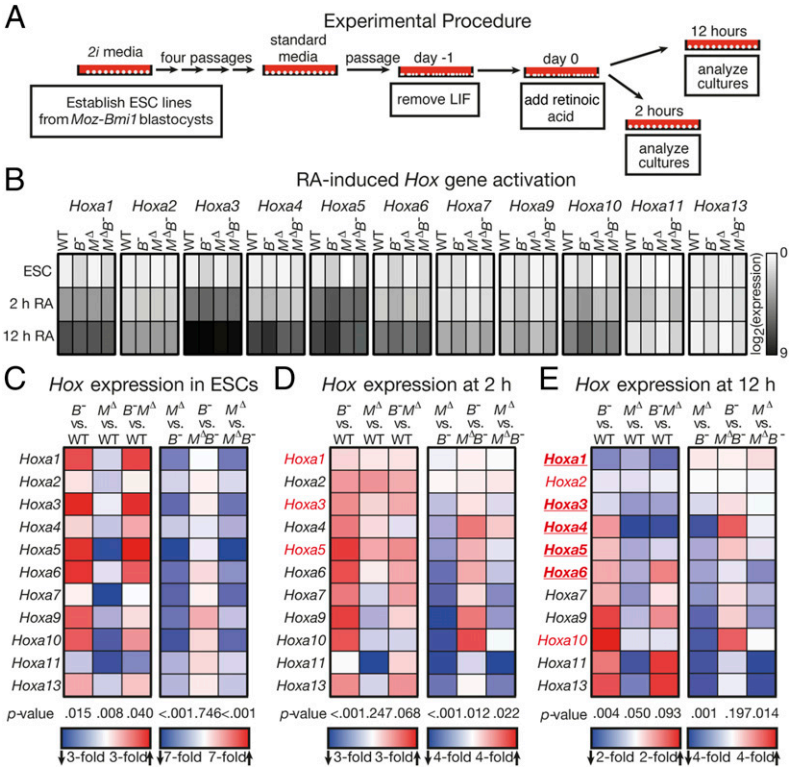

Fig. 2. MOZ and BMI1 play opposing roles during *Hox* gene activation. (*A*) Experimental time course of *Hox* gene induction in embryonic stem cells (ES cell) using retinoic acid (RA). (*B*) *Hox* gene expression in undifferentiated ES cells (ESC; day −1), as well as after two and twelve hours of treatment with 20 nM RA. (*C*) Relative *Hox* gene expression in undifferentiated ES cell lines (ESC) cultured with LIF. (*D*) Relative *Hox* gene expression in ES cells after treatment with 20 nM RA for two hours. *Hox* genes highlighted in red (*Hoxa1*, *Hoxa3*, and *Hoxa5*) were activated 10- to 20-fold over basal levels in ES cells. (*E*) *Hox* gene expression levels following 12 h of 20 nM RA treatment. *Hox* genes highlighted in red showed a 10- to 20-fold increase in *Hox* mRNA levels compared with undifferentiated ES cells, whereas *Hox* genes highlighted in red and underlined showed a 20- to 200-fold increase. Data are presented as mean ± SEM. *Hox* mRNA was normalized to expression of house keeping genes *Hsp90ab1* and *Gapdh*. $n = 3$ wild type, 3 $Bmi1^{-/-}$, 2 $Moz^{\Delta/\Delta}$, and 3 $Moz^{\Delta/\Delta}$;$Bmi1^{-/-}$ independent ES cell lines for all panels. *P* values for overall changes in *HoxA* cluster gene expression are indicated below the heat map in *C*–*E*. See related data in *SI Appendix*, Fig. S2.

significantly higher levels in $Bmi1^{-/-}$ cells (Fig. 2*D*, $P < 0.001$). In contrast, the effect of MOZ-deficiency was no longer evident, with similar *HoxA* cluster expression observed in $Moz^{\Delta/\Delta}$ and wild type ($P = 0.247$). Nevertheless, we observed that in contrast to undifferentiated ES cells (Fig. 2*C*), *HoxA* cluster expression was similar between $Moz^{\Delta/\Delta}$;$Bmi1^{-/-}$ and wild type cells after two hours of RA treatment (Fig. 2*D*, $P = 0.068$). Indeed, after two hours of RA-treatment, $Moz^{\Delta/\Delta}$;$Bmi1^{-/-}$ cells showed intermediate *HoxA* gene expression levels compared with cells singly deficient in MOZ or in BMI1, i.e., significantly lower than $Bmi1^{-/-}$ cells (Fig. 2*D*, $P = 0.022$) and significantly higher than $Moz^{\Delta/\Delta}$ cells ($P = 0.012$). These data suggest that the effects of MOZ and BMI1 on *Hox* gene expression levels were in balance after two hours of RA treatment, concurrent with the earliest phase of *Hox* gene activation.

MOZ Is Required to Maintain Normal *Hox* mRNA Levels in Differentiating ES Cells. To obtain insights into the maintenance of *Hox* gene mRNA by MOZ and BMI1, we analyzed cells that had been treated with RA for 12 h. At the 12-h time-point, the first six *HoxA* cluster genes were strongly expressed (Fig. 2*E*). Although overall *HoxA* cluster mRNA was still more abundant in $Bmi1^{-/-}$ cells compared with wild type ($P = 0.004$), the strongly active *Hox* genes, *Hoxa1* to *Hoxa6*, were no longer expressed at higher levels compared with wild type (Fig. 2*E*, $P = 0.355$). Those *Hox* genes that were yet to be strongly activated, *Hoxa7* to *Hoxa13*, were still affected by the loss of BMI1 and showed higher expression compared with wild type ($P = 0.002$). These findings suggest that BMI1 is particularly important for restraining expression of *Hox* genes before activation, but not necessarily important for maintaining their mRNA levels, once *Hox* genes have been strongly induced.

In contrast to $Bmi1^{-/-}$, all *HoxA* gene expression levels were lower in $Moz^{\Delta/\Delta}$ cells after 12 h of RA induction (Fig. 2*E*, $P = 0.05$). This was consistent with low levels of *Hox* gene expression in $Moz^{\Delta/\Delta}$ E10.5 embryo (13) and in undifferentiated ES cells (Fig. 2*C*). Interestingly, a combination of $Moz^{\Delta/\Delta}$ and $Bmi1^{-/-}$ effects were seen in $Moz^{\Delta/\Delta}$;$Bmi1^{-/-}$ cells. As evident in Fig. 2*E*, the *Hox* cluster separated into two domains in $Moz^{\Delta/\Delta}$;$Bmi1^{-/-}$ cells. The first domain, the strongly activated genes *Hoxa1* to *Hoxa5*, showed a $Moz^{\Delta/\Delta}$ like phenotype with low expression levels (Fig. 2*E*, $Moz^{\Delta/\Delta}$;$Bmi1^{-/-}$ panel). In contrast, the second domain, the more 5′ genes *Hoxa7* to *Hoxa13*, which were yet to be strongly activated, showed a $Bmi1^{-/-}$ like phenotype and were expressed at higher levels compared with wild type ($P = 0.014$) and $Moz^{\Delta/\Delta}$ cells ($P = 0.007$). These data suggest that MOZ is important for maintaining normal levels of *Hox* mRNA after the initial activation of *Hox* gene transcription.

Together, our analyses in ES cells suggest that BMI1 is required to prevent premature activation of *Hox* genes and that MOZ and BMI1 play opposing roles during the early RA-induced *Hox* gene activation phase. In addition, we find that MOZ, but not BMI1, is required to maintain normal levels of mRNA after the initial activation phase.

MOZ, but Not BMI1, Is Required to Maintain Normal *Hox* mRNA Levels in E10.5 Embryos. Our experiments involving differentiation of *Moz*;*Bmi1* ES cells suggested that MOZ, but not BMI1, was required to maintain normal levels of *Hox* mRNA after their initial activation. Although these data are consistent with the

DEVELOPMENTAL BIOLOGY

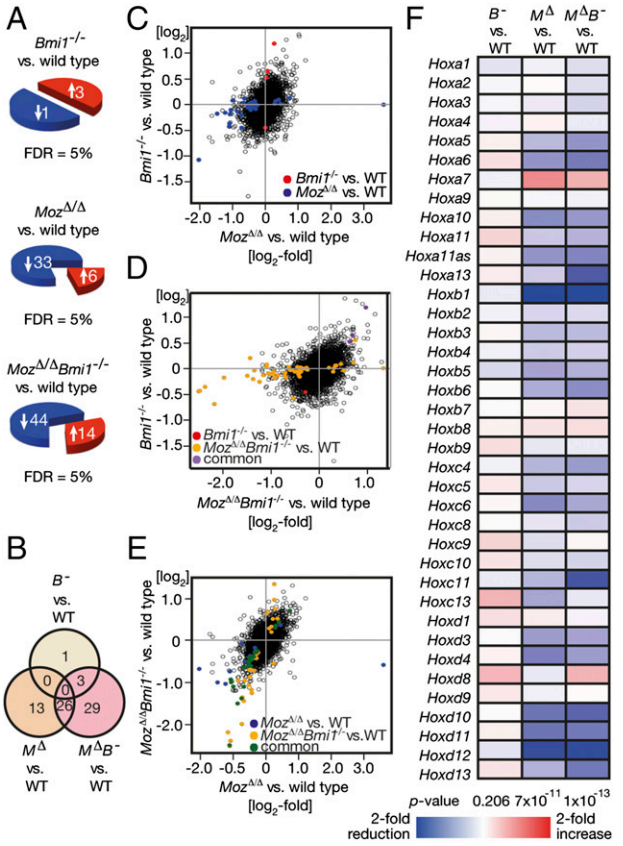

Fig. 3. MOZ, but not BMI1, is required for normal *Hox* gene expression levels at E10.5. (*A*) Number of differentially expressed genes in $Bmi1^{-/-}$, $Moz^{\Delta/\Delta}$, and $Moz^{\Delta/\Delta}$;$Bmi1^{-/-}$ embryos relative to wild type. (*B*) Venn diagram showing overlap in differentially expressed genes in single and double *Moz* and *Bmi1* knockout embryos. (*C*–*E*) Correlation of differential expression. Colored circles depict genes that are significantly changed, open circles, not significant. (*F*) Heat map depicting *Hox* gene expression levels in $Bmi1^{-/-}$, $Moz^{\Delta/\Delta}$, and $Moz^{\Delta/\Delta}$;$Bmi1^{-/-}$ embryos relative to wild type. $n = 3$ embryos per genotype in all panels. False discovery rate is 5% in *A* and *B* and 20% in *C*–*E*.

reduction of *Hox* gene mRNA in $Moz^{\Delta/\Delta}$ embryos (13), studies using mouse fibroblasts and HeLa cell lines have suggested that there is a continued requirement for BMI1 to maintain *Hox* gene silencing in mammalian cells (14, 17). Given these contradictions, we assayed *Hox* mRNA levels in whole stage-matched E10.5 embryos by RNA-sequencing (Fig. 3 and *SI Appendix*, Fig. S3 and Table S2).

With a false discovery rate (FDR) of 5% (equivalent to *p*-value cutoff of 2.1×10^{-4}), only 4 genes were differentially expressed in $Bmi1^{-/-}$ embryos including *Bmi1* itself (Fig. 3 *A* and *B* and *SI Appendix*, Table S3). In comparison, 33 genes were down-regulated and 6 up-regulated in $Moz^{\Delta/\Delta}$ embryos compared with wild type (*SI Appendix*, Table S3), and 44 genes down-regulated and 14 up-regulated in $Moz^{\Delta/\Delta}$;$Bmi1^{-/-}$ embryos (*SI Appendix*, Table S3). Even when the FDR cutoff was relaxed to 20% (equivalent to *P* value cutoff of 0.001), BMI1 did not have a significant effect on gene transcription levels compared with MOZ (Fig. 3 *C* and *D*). This trend extended to *Hox* genes. Consistent with our ES cell-differentiation results (Fig. 2*E*), BMI1-deficiency had no significant effect on the levels of *Hox* gene expression in the E10.5 embryos (Fig. 3*F*, $P = 0.206$). In contrast, *Hox* genes were significantly down-regulated in $Moz^{\Delta/\Delta}$ E10.5 embryos ($P = 7 \times 10^{-11}$). Consistent with the strong effect of *Moz*-deletion and the lack of influence of *Bmi1*-deletion on *Hox* mRNA levels, *Hox* gene expression was low in $Moz^{\Delta/\Delta}$;$Bmi1^{-/-}$ embryos ($P = 1 \times 10^{-13}$).

The gene expression analysis presented here (Fig. 3), along with our analyses of differentiating *Moz*;*Bmi1* ES cells (Fig. 2), provide strong evidence that once *Hox* genes have been activated, MOZ is required to maintain their normal expression levels. In contrast, BMI1 does not appear to be critical for the regulation of mRNA levels during the maintenance phase.

MOZ and BMI1 Play Opposing Roles in Regulating Body Segment Identity. *Hox* genes play a critical role in specifying body segment identity in the anterior–posterior axis (1). To interrogate the relationship between *Moz* and *Bmi1* in vivo, we wanted to determine if the anterior–posterior patterning defects observed in single $Moz^{\Delta/\Delta}$ and $Bmi1^{-/-}$ mutants were rescued in $Moz^{\Delta/\Delta}$;$Bmi1^{-/-}$ animals. Thus, we isolated *Moz*;*Bmi1* compound knockout animals between E15.5 and E18.5 and interrogated the axial skeleton for shifts in body segment identity.

Wild type mice possess a complement of 7 cervical, 13 thoracic, 6 lumbar and 4 sacral vertebrae (Fig. 4 *A* and *E* and *SI Appendix*, Fig. S4 *A* and *E*). Consistent with the initial description of the $Bmi1^{-/-}$ phenotype (23), 56% of $Bmi1^{-/-}$ pups ($n = 14/25$) presented with posterior homeotic transformations (Fig. 4*B*). For instance, a C1 to C2 transformation was present in $Bmi1^{-/-}$ fetuses, as evident by the lack of the anterior arch of the atlas (aaa), which is normally observed associated with the C1 segment. Furthermore, the C2′ vertebra in $Bmi1^{-/-}$ pups resembled the wild type C3 segment and this shift in identity was perpetuated throughout the entire length of the axial skeleton (Fig. 4*E* and *SI Appendix*, Fig. S4 *B* and *F*). In contrast, all $Moz^{\Delta/\Delta}$ pups presented with an anterior shift in body segment identity ($n = 17/17$), which was consistent with our previous observations (13). Although the C1 vertebra was normal in $Moz^{\Delta/\Delta}$ animals, the second vertebra (C2′) had a C1-like identity (Fig. 4*C* and *SI Appendix*, Fig. S4*C*). The C3′ to C8′ segments of $Moz^{\Delta/\Delta}$ pups were phenotypically

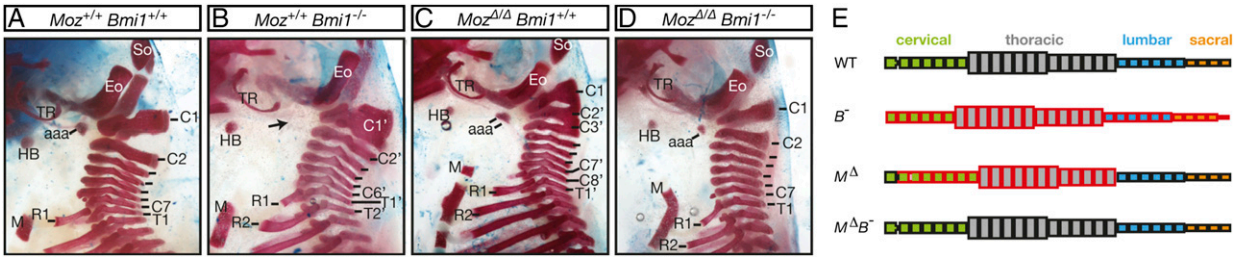

Fig. 4. MOZ and BMI1 play opposing roles in regulating body segment identity. (*A*–*D*) Representative skeletal preparations of wild type, $Bmi1^{-/-}$, $Moz^{\Delta/\Delta}$, and $Moz^{\Delta/\Delta}$;$Bmi1^{-/-}$ E18.5 pups. The arrow in *B* marks the absence of the anterior arch of the atlas (aaa). Apostrophes indicate a shift in body segment identity. Note the posterior shift in segment identity in $Bmi1^{-/-}$ pups (*B*) and the anterior shift in $Moz^{\Delta/\Delta}$ animals (*C*), which were rescued to a wild type phenotype in $Moz^{\Delta/\Delta}$;$Bmi1^{-/-}$ pups (*D*). (*E*) Schematic representation of homeotic transformations (red outline). See related data in *SI Appendix*, Fig. S4 and Table S4. aaa, anterior arch of the atlas; C, cervical vertebrae; Eo, exooccipital bone; HB, hyoid bone; M, manubrium sterni; R, rib; So, supraoccipital bone; T, thoracic vertebrae; TR, tympanic ring. $n = 16$ WT, 25 $Bmi1^{-/-}$, 17 $Moz^{\Delta/\Delta}$ and 14 $Moz^{\Delta/\Delta}$;$Bmi1^{-/-}$.

similar to wild-type segments C2 to C7 (*SI Appendix*, Fig. S4*C*). This anterior shift in body segment identity in $Moz^{\Delta/\Delta}$ animals was perpetuated for 19 vertebral segments from C2 to T13 (Fig. 4*E* and *SI Appendix*, Fig. S4*G*).

Remarkably, 93% of $Moz^{\Delta/\Delta}$;$Bmi1^{-/-}$ fetuses (n = 13/14) showed restoration of the axial skeleton (Fig. 4*D* and *SI Appendix*, Fig. S4 *D* and *H*). The first cervical segment had an anterior arch of the atlas (Fig. 4*D*). Furthermore, the next six segments (C2 to C7) in $Moz^{\Delta/\Delta}$;$Bmi1^{-/-}$ pups closely resembled that of wild type C2 to C7 segments (*SI Appendix*, Fig. S4*D*). This normal identity was preserved along the entire axial skeleton in $Moz^{\Delta/\Delta}$;$Bmi1^{-/-}$ animals (Fig. 4*E* and *SI Appendix*, Fig. S4*H*). Thus, the body segment identity defects in single $Moz^{\Delta/\Delta}$ pups and in $Bmi1^{-/-}$ pups were rescued toward a wild type identity in $Moz^{\Delta/\Delta}$;$Bmi1^{-/-}$ animals (Fig. 4 and *SI Appendix*, Fig. S4 and Table S4).

MOZ and BMI1 Play Opposing Roles in Regulating the Anterior Expression Boundary of *Hox* Genes. We have established that the simultaneous deletion of *Moz* and *Bmi1* largely rescued the defects in body segment identity observed in the single $Moz^{\Delta/\Delta}$ and $Bmi1^{-/-}$ mutant animals. Because *Hox* gene expression boundaries specify body segment identity, we investigated whether the *Hox* gene expression boundaries were also restored to a wild type location in $Moz^{\Delta/\Delta}$;$Bmi1^{-/-}$ animals. Thus, we analyzed the expression of *Hoxc5* and *Hoxa9* mRNA via whole mount in situ hybridization, and HOXB4 protein by whole mount immunohistochemistry in E10.5 embryos.

In wild type E10.5 embryos, the anterior limit of *Hoxc5* expression was clearly evident in the neural tube (Fig. 5*A*). In $Bmi1^{-/-}$ mutants (n = 3/4), an anterior shift in the *Hoxc5* expression boundary was observed (Fig. 5*B*), whereas in $Moz^{\Delta/\Delta}$ embryos (n = 4/4), a posterior shift in *Hoxc5* expression was evident (Fig. 5*C*). These shifts in the anterior expression boundary of *Hoxc5* observed in single $Moz^{\Delta/\Delta}$ and $Bmi1^{-/-}$ mutants were rescued to the wild type location in $Moz^{\Delta/\Delta}$;$Bmi1^{-/-}$ embryos (n = 3/4, Fig. 5*D* and *SI Appendix*, Fig. S5 and Table S5). Similarly, the anterior shifts in the expression of *Hoxa9* mRNA and HOXB4 protein in $Bmi1^{-/-}$, and the posterior shifts in $Moz^{\Delta/\Delta}$ E10.5 embryos, were rescued to a wild type phenotype in $Moz^{\Delta/\Delta}$;$Bmi1^{-/-}$ embryos (*SI Appendix*, Figs. S6–S8 and Table S5).

These analyses revealed that MOZ and BMI1 play opposing roles in regulating the anterior expression boundaries of *Hox* genes during development (*SI Appendix*, Table S5). These data are consistent with the opposing roles of MOZ and BMI1 in regulating body segment identity in vivo (Fig. 4).

Discussion

In the current study, we set out to investigate the importance of chromatin modifying complexes during the activation phase of *Hox* gene expression. Through the systematic analysis of early events during ES cell differentiation, we establish that MOZ and BMI1 play opposing roles during the activation phase of *Hox* genes. Given the strong correlation between *Hox* gene expression and the location of cells in the anterior–posterior axis (28), we further analyzed the relationship of MOZ and BMI1 in specifying segment identity along the anterior–posterior body axis in vivo. We found that during embryogenesis, MOZ and BMI1 played opposing roles in specifying *Hox* gene expression boundaries and body segment identity in vivo.

Hox genes were first discovered in *Drosophila*, where mutations in *homeotic* genes led to homeotic transformations (29–31). The *homeotic* gene expression domains in *Drosophila* are thought to be setup by the initial deposition of maternal mRNAs in the oocyte, and the subsequent action of gap and pair-rule transcription factors (32). The action of these transcription factors is only transient. The *Drosophila* polycomb and trithorax group (homolog of mammalian MLL) proteins are thought to maintain the *homeotic* gene expression patterns, once they have been established (reviewed by ref. 33). Based on findings in *Drosophila*, early studies on mammalian counterparts of polycomb and trithorax group proteins also suggested that these complexes are important for the maintenance, but not the initiation of *Hox* gene expression (11, 12). However, the process of *Hox* gene activation and spatial specification of *Hox* gene expression in the mouse differs considerably to that in *Drosophila*. The homologs of *Drosophila* gap and pair-rule genes do not appear to play a systematic role in *Hox* gene activation in mice. Rather, other mechanisms appear to be at play in vertebrates, including specific transcription factors, fibroblast growth factor and RA signaling (34–39). Moreover, although collinearity between genomic order and spatial expression pattern is conserved between the two species, *Hox* genes are activated additionally in a temporally collinear manner in mice (4). In vertebrates, the eventual destination of cells along the anterior-to-posterior axis depends on the transcriptional status of their *Hox* loci before they ingress from the epiblast into the primitive streak (28). In light of this literature and our data presented in this study, we propose that homeotic transformations in $Moz^{\Delta/\Delta}$ and $Bmi1^{-/-}$ single mutant animals occur due to opposing defects during the transition of *Hox* loci from the transcriptionally repressed to the active state. In this model, premature activation in BMI1-deficient animals, or delayed activation of *Hox* genes in the MOZ-deficient state, leads to homeotic transformations. Consistent with this hypothesis, we find that defects observed during the onset of *Hox* gene expression in $Moz^{\Delta/\Delta}$ and $Bmi1^{-/-}$ single knockout ES cells were normalized by the combined deletion of *Moz* and *Bmi1*.

A number of in vitro studies have proposed a continued requirement for BMI1 to maintain *Hox* genes in a transcriptionally silent state (14, 17). However, in contrast to MOZ, we could not find any evidence for an effect of BMI1 on *Hox* gene mRNA levels in E10.5 embryos or in differentiating ES cells. Although we cannot rule out that BMI1 prevents the excessive spread of *Hox* gene expression domains after their initial activation, or that homologs of BMI1 may play an important role in the maintenance phase of *Hox* gene expression, our data argue against a role for BMI1 in maintaining *Hox* gene mRNA levels. Foremost, we detect *Bmi1* mRNA expression in the primitive steak in E7.5 embryos, a time correlated with *Hox* gene activation (Fig. 1). In contrast, only low levels of *Bmi1* mRNA were detected in the E10.5 embryo (Fig. 1), a stage correlating with the maintenance of *Hox* gene expression. Furthermore, although *Bmi1*-deletion resulted in increased and premature *Hox* gene expression in ES cells before differentiation, we found no significant changes in mRNA levels of strongly activated *Hox* genes in RA-treated $Bmi1^{-/-}$ ES cells or $Bmi1^{-/-}$ E10.5 embryos (Figs. 2 and 3). In fact, these data further suggest that the timely activation of *Hox* genes is important for the correct patterning of the anterior–posterior axis as opposed to absolute *Hox* mRNA levels. For instance, *Hox* mRNA levels in E10.5 $Moz^{\Delta/\Delta}$;$Bmi1^{-/-}$ embryos were low and similar to $Moz^{\Delta/\Delta}$ embryos, whereas body segment identity was largely rescued. In agreement with this interpretation of our data,

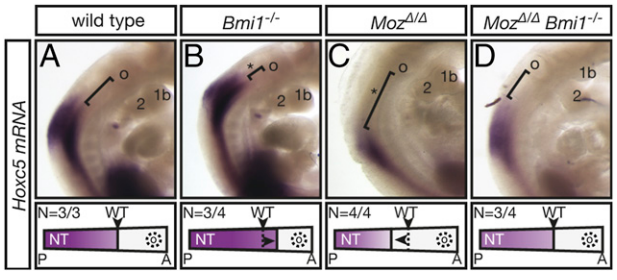

Fig. 5. MOZ and BMI1 play opposing roles in specifying anterior *Hox* gene expression boundaries. (*A–D*) *Hoxc5* mRNA expression in E10.5 embryos. Shifts in the rostral *Hoxc5* expression boundary in the neural tube are shown relative to the otic vesicle (o). See related data in *SI Appendix*, Figs. S5–S8 and Table S5. n = number of individual embryos stated in *A–D*. Schematics below images show the most common expression boundary observed. A, anterior; NT, neural tube; P, posterior.

there is increasing evidence that the timely activation of *Hox* genes is critical for proper anterior–posterior patterning (see review by ref. 40). For instance, deletion of the *Hoxc8* enhancer (41), or deletion of the *Hoxd10* enhancer (42), leads to a temporal delay in activation of the respective *Hox* gene and anterior shifts in body segment identity. We propose here that MOZ and BMI1 bestow proper patterning of the anterior–posterior axis by ensuring the timely transition of *Hox* loci from a repressed to an active state.

We show in this study that MOZ and BMI1 play a particularly important and previously unappreciated role during the initial activation phase of *Hox* gene expression in the ES cell model. This correlates with their opposing role in correctly specifying body segment identity in the anterior–posterior axis during embryogenesis. Extrapolating from our ES cell culture findings, we propose that the actions of the chromatin modifying complexes containing MOZ and BMI1 during the early activation phase of *Hox* genes is critical for the correct specification of body segment identity.

Materials and Methods

Mice were maintained on a mixed *FVB/BALB/c* background. The Moz^{Δ} allele (25) and the $Bmi1^{-}$ mutant allele (23) have been previously described. For timed matings, the morning that a vaginal plug was observed was designated as E0.5. All experiments were performed under approval from the Walter and Eliza Hall Institute's Animal Ethics Committee and conformed to the Australian code of practice for the care and use of animals for scientific purposes. The number of observations (N) stated for each experiment represents biological replicates (individual embryos or cell isolates from individual embryos) and not technical replicates.

Skeletal preparations of fetuses aged between E15.5 and E18.5 were processed and stained with Alizarin red for bone and Alcian blue for cartilage components as previously described (43). Whole mount in situ hybridization (44) and whole mount immunohistochemistry (24) was conducted as previously described. ES cell culture was carried out as described (13). All data are presented as mean ± SEM. Statistical analyses were carried out using Stata/IC v12 (Stata Corporation, USA), unless further specified in the SI. Data were analyzed using one-factorial ANOVA, with *Moz;Bmi1* genotype as the independent variable, followed by Bonferroni's post hoc test.

Details are provided in the *SI Appendix, SI Materials and Methods*.

ACKNOWLEDGMENTS. We thank M. van Lohuizen for the *Bmi1* mutant mice and are grateful to R. Cobb, C. Gatt, and F. Dabrowski for excellent technical support. This work was funded by Australian National Health and Medical Research Council (NHMRC) Project Grants 1010851, 1008699, 1030704 and 1051078, NHMRC Research Fellowships [1058892 (to G.K.S.), 1003435 (to T.T.), and 575512 and 1081421 (to A.K.V.)], NHMRC Dora Lush Scholarship (BNS), Australian Postgraduate Award (to H.K.V.), International Postgraduate Research Scholarship (A.J.K.), NHMRC Independent Research Institutes Infrastructure Support (IRIIS) Scheme and a Victorian State Government Operational Infrastructure Support (OIS) Grant.

1. Garcia-Fernàndez J (2005) The genesis and evolution of homeobox gene clusters. *Nat Rev Genet* 6(12):881–892.
2. Graham A, Papalopulu N, Krumlauf R (1989) The murine and Drosophila homeobox gene complexes have common features of organization and expression. *Cell* 57(3): 367–378.
3. Izpisúa-Belmonte JC, Falkenstein H, Dollé P, Renucci A, Duboule D (1991) Murine genes related to the Drosophila AbdB homeotic genes are sequentially expressed during development of the posterior part of the body. *EMBO J* 10(8):2279–2289.
4. Duboule D (1994) Temporal colinearity and the phylotypic progression: A basis for the stability of a vertebrate Bauplan and the evolution of morphologies through heterochrony. *Dev Suppl* 135–142.
5. Deschamps J, et al. (1999) Initiation, establishment and maintenance of Hox gene expression patterns in the mouse. *Int J Dev Biol* 43(7):635–650.
6. Noordermeer D, et al. (2014) Temporal dynamics and developmental memory of 3D chromatin architecture at Hox gene loci. *eLife* 3:e02557.
7. Bernstein BE, et al. (2006) A bivalent chromatin structure marks key developmental genes in embryonic stem cells. *Cell* 125(2):315–326.
8. Mikkelsen TS, et al. (2007) Genome-wide maps of chromatin state in pluripotent and lineage-committed cells. *Nature* 448(7153):553–560.
9. Soshnikova N, Duboule D (2009) Epigenetic temporal control of mouse Hox genes in vivo. *Science* 324(5932):1320–1323.
10. Noordermeer D, et al. (2011) The dynamic architecture of Hox gene clusters. *Science* 334(6053):222–225.
11. Akasaka T, et al. (2001) Mice doubly deficient for the Polycomb Group genes Mel18 and Bmi1 reveal synergy and requirement for maintenance but not initiation of Hox gene expression. *Development* 128(9):1587–1597.
12. Yu BD, Hanson RD, Hess JL, Horning SE, Korsmeyer SJ (1998) MLL, a mammalian trithorax-group gene, functions as a transcriptional maintenance factor in morphogenesis. *Proc Natl Acad Sci USA* 95(18):10632–10636.
13. Voss AK, Collin C, Dixon MP, Thomas T (2009) Moz and retinoic acid coordinately regulate H3K9 acetylation, Hox gene expression, and segment identity. *Dev Cell* 17(5): 674–686.
14. Cao R, Tsukada Y, Zhang Y (2005) Role of Bmi-1 and Ring1A in H2A ubiquitylation and Hox gene silencing. *Mol Cell* 20(6):845–854.
15. Doyon Y, et al. (2006) ING tumor suppressor proteins are critical regulators of chromatin acetylation required for genome expression and perpetuation. *Mol Cell* 21(1): 51–64.
16. Ullah M, et al. (2008) Molecular architecture of quartet MOZ/MORF histone acetyltransferase complexes. *Mol Cell Biol* 28(22):6828–6843.
17. Wei J, Zhai L, Xu J, Wang H (2006) Role of Bmi1 in H2A ubiquitylation and Hox gene silencing. *J Biol Chem* 281(32):22537–22544.
18. Buchwald G, et al. (2006) Structure and E3-ligase activity of the Ring-Ring complex of polycomb proteins Bmi1 and Ring1b. *EMBO J* 25(11):2465–2474.
19. Endoh M, et al. (2012) Histone H2A mono-ubiquitination is a crucial step to mediate PRC1-dependent repression of developmental genes to maintain ES cell identity. *PLoS Genet* 8(7):e1002774.
20. Stock JK, et al. (2007) Ring1-mediated ubiquitination of H2A restrains poised RNA polymerase II at bivalent genes in mouse ES cells. *Nat Cell Biol* 9(12):1428–1435.
21. Eskeland R, et al. (2010) Ring1B compacts chromatin structure and represses gene expression independent of histone ubiquitination. *Mol Cell* 38(3):452–464.
22. van der Lugt NM, Alkema M, Berns A, Deschamps J (1996) The Polycomb-group homolog Bmi-1 is a regulator of murine Hox gene expression. *Mech Dev* 58(1-2): 153–164.
23. van der Lugt NM, et al. (1994) Posterior transformation, neurological abnormalities, and severe hematopoietic defects in mice with a targeted deletion of the bmi-1 proto-oncogene. *Genes Dev* 8(7):757–769.
24. Voss AK, et al. (2012) MOZ regulates the Tbx1 locus, and Moz mutation partially phenocopies DiGeorge syndrome. *Dev Cell* 23(3):652–663.
25. Thomas T, et al. (2006) Monocytic leukemia zinc finger protein is essential for the development of long-term reconstituting hematopoietic stem cells. *Genes Dev* 20(9): 1175–1186.
26. Pelletier N, Champagne N, Stifani S, Yang XJ (2002) MOZ and MORF histone acetyltransferases interact with the Runt-domain transcription factor Runx2. *Oncogene* 21(17):2729–2740.
27. Sheikh BN, Downer NL, Kueh AJ, Thomas T, Voss AK (2014) Excessive versus physiologically relevant levels of retinoic acid in embryonic stem cell differentiation. *Stem Cells* 32(6):1451–1458.
28. Iimura T, Pourquié O (2006) Collinear activation of Hoxb genes during gastrulation is linked to mesoderm cell ingression. *Nature* 442(7102):568–571.
29. Lewis EB (1978) A gene complex controlling segmentation in Drosophila. *Nature* 276(5688):565–570.
30. Scott MP, et al. (1983) The molecular organization of the Antennapedia locus of Drosophila. *Cell* 35(3 Pt 2):763–776.
31. Bender W, et al. (1983) Molecular Genetics of the Bithorax Complex in Drosophila melanogaster. *Science* 221(4605):23–29.
32. Peel AD, Chipman AD, Akam M (2005) Arthropod segmentation: Beyond the Drosophila paradigm. *Nat Rev Genet* 6(12):905–916.
33. Schuettengruber B, Chourrout D, Vervoort M, Leblanc B, Cavalli G (2007) Genome regulation by polycomb and trithorax proteins. *Cell* 128(4):735–745.
34. Marshall H, et al. (1994) A conserved retinoic acid response element required for early expression of the homeobox gene Hoxb-1. *Nature* 370(6490):567–571.
35. Sham MH, et al. (1993) The zinc finger gene Krox20 regulates HoxB2 (Hox2.8) during hindbrain segmentation. *Cell* 72(2):183–196.
36. Manzanares M, et al. (1997) Segmental regulation of Hoxb-3 by kreisler. *Nature* 387(6629):191–195.
37. Dubrulle J, McGrew MJ, Pourquié O (2001) FGF signaling controls somite boundary position and regulates segmentation clock control of spatiotemporal Hox gene activation. *Cell* 106(2):219–232.
38. Gould A, Itasaki N, Krumlauf R (1998) Initiation of rhombomeric Hoxb4 expression requires induction by somites and a retinoid pathway. *Neuron* 21(1):39–51.
39. Cunningham TJ, Duester G (2015) Mechanisms of retinoic acid signalling and its roles in organ and limb development. *Nat Rev Mol Cell Biol* 16(2):110–123.
40. Casaca A, Santos AC, Mallo M (2014) Controlling Hox gene expression and activity to build the vertebrate axial skeleton. *Dev Dyn* 243(1):24–36.
41. Juan AH, Ruddle FH (2003) Enhancer timing of Hox gene expression: Deletion of the endogenous Hoxc8 early enhancer. *Development* 130(20):4823–4834.
42. Zákány J, Gérard M, Favier B, Duboule D (1997) Deletion of a HoxD enhancer induces transcriptional heterochrony leading to transposition of the sacrum. *EMBO J* 16(14): 4393–4402.
43. Thomas T, Voss AK, Chowdhury K, Gruss P (2000) Querkopf, a MYST family histone acetyltransferase, is required for normal cerebral cortex development. *Development* 127(12):2537–2548.
44. Thomas T, Loveland KL, Voss AK (2007) The genes coding for the MYST family histone acetyltransferases, Tip60 and Mof, are expressed at high levels during sperm development. *Gene Expr Patterns* 7(6):657–665.